

# Supplementary Material: Polarization Demosaicking for Monochrome and Color Polarization Focal Plane Arrays

Simeng Qiu , Qiang Fu , Congli Wang and Wolfgang Heidrich

King Abdullah University of Science and Technology (KAUST), Saudi Arabia

## 1. Stokes Vector and Müller Matrix

For completeness, we cover the fundamentals of Stokes vector and Müller matrix here. Detailed derivations can be found in [Col05].

Stokes vector is a representation of polarization states for incoherent light. By definition, completely unpolarized light can be expressed as  $\mathbf{S}_{\text{up}} = [1, 0, 0]^T$ . The Stokes vectors for typical polarization angles  $0^\circ$ ,  $45^\circ$ ,  $90^\circ$  and  $135^\circ$  with unit total intensity are shown in Eq. (1).

$$\mathbf{S}_0 = \begin{bmatrix} 1 \\ 1 \\ 0 \\ 0 \end{bmatrix}, \mathbf{S}_{45} = \begin{bmatrix} 1 \\ 0 \\ 1 \\ 0 \end{bmatrix}, \mathbf{S}_{90} = \begin{bmatrix} 1 \\ -1 \\ 0 \\ 0 \end{bmatrix}, \mathbf{S}_{135} = \begin{bmatrix} 1 \\ 0 \\ -1 \\ 0 \end{bmatrix}. \quad (1)$$

The polarization property of an optical element is characterized by its Müller matrix, which consists of  $3 \times 3$  entries. For example, an ideal linear horizontal polarizer converts completely unpolarized light into horizontally polarized light. In general, the Müller matrix for an ideal linear polarizer oriented  $\theta$  with respect to horizon is

$$\mathbf{M}_\theta = \frac{1}{2} \begin{bmatrix} 1 & \cos(2\theta) & \sin(2\theta) \\ \cos(2\theta) & \cos^2(2\theta) & \sin(2\theta)\cos(2\theta) \\ \sin(2\theta) & \sin(2\theta)\cos(2\theta) & \sin^2(2\theta) \end{bmatrix}. \quad (2)$$

So the Müller matrices for  $0^\circ$ ,  $45^\circ$ ,  $90^\circ$  and  $135^\circ$  polarizers are

$$\left\{ \begin{array}{l} \mathbf{M}_0 = \frac{1}{2} \begin{bmatrix} 1 & 1 & 0 \\ 1 & 1 & 0 \\ 0 & 0 & 0 \end{bmatrix}, \quad \mathbf{M}_{90} = \frac{1}{2} \begin{bmatrix} 1 & -1 & 0 \\ -1 & 1 & 0 \\ 0 & 0 & 0 \end{bmatrix} \\ \mathbf{M}_{45} = \frac{1}{2} \begin{bmatrix} 1 & 0 & 1 \\ 0 & 0 & 0 \\ 1 & 0 & 1 \end{bmatrix}, \quad \mathbf{M}_{135} = \frac{1}{2} \begin{bmatrix} 1 & 0 & -1 \\ 0 & 0 & 0 \\ -1 & 0 & 1 \end{bmatrix} \end{array} \right. \quad (3)$$

An ideal polarizer can transmit all the light parallel to its orientation angle, and block light completely in the perpendicular direction. In reality, fabrication artifacts lead to imperfections on the polarizer. The parallel (major) transmittance and perpendicular (minor) transmittance become  $k_1$  and  $k_2$ , where  $0 \leq k_1, k_2 \leq 1$ . Diattenuation is defined as

$$D = \frac{k_1 + k_2}{k_1 - k_2}, \quad (4)$$

and extinction ratio is defined as

$$\text{ER} = \frac{k_1}{k_2} = \frac{D+1}{D-1}. \quad (5)$$

The Müller matrices for the above polarizers are now

$$\left\{ \begin{array}{l} \mathbf{M}_0 = \frac{1}{2} \begin{bmatrix} k_1^0 + k_2^0 & k_1^0 - k_2^0 & 0 \\ k_1^0 - k_2^0 & k_1^0 + k_2^0 & 0 \\ 0 & 0 & 0 \end{bmatrix} \\ \mathbf{M}_{45} = \frac{1}{2} \begin{bmatrix} k_1^{45} + k_2^{45} & 0 & k_1^{45} - k_2^{45} \\ 0 & 0 & 0 \\ k_1^{45} + k_2^{45} & 0 & k_1^{45} - k_2^{45} \end{bmatrix} \\ \mathbf{M}_{90} = \frac{1}{2} \begin{bmatrix} k_1^{90} + k_2^{90} & -\left(k_1^{90} - k_2^{90}\right) & 0 \\ -\left(k_1^{90} - k_2^{90}\right) & k_1^{90} + k_2^{90} & 0 \\ 0 & 0 & 0 \end{bmatrix} \\ \mathbf{M}_{135} = \frac{1}{2} \begin{bmatrix} k_1^{135} + k_2^{135} & 0 & -\left(k_1^{135} + k_2^{135}\right) \\ 0 & 0 & 0 \\ -\left(k_1^{135} - k_2^{135}\right) & 0 & k_1^{135} + k_2^{135} \end{bmatrix} \end{array} \right. \quad (6)$$

Since the sensor can only measure the intensity, for each super pixel in the polarization sensor, the captured intensities for  $0^\circ$ ,  $45^\circ$ ,  $90^\circ$  and  $135^\circ$  can be obtained from the Stokes vector as follows.

$$\begin{bmatrix} I_0 \\ I_{45} \\ I_{90} \\ I_{135} \end{bmatrix} = \frac{1}{2} \begin{bmatrix} 1 & 1 & 0 \\ 1 & 0 & 1 \\ 1 & -1 & 0 \\ 1 & 0 & -1 \end{bmatrix} \begin{bmatrix} S_0 \\ S_1 \\ S_2 \end{bmatrix}. \quad (7)$$

On the other hand, the conversion from the four intensities to Stokes vector can also be written in the matrix-vector product form by

$$\begin{aligned} \begin{bmatrix} S_0 \\ S_1 \\ S_2 \end{bmatrix} &= \begin{bmatrix} 1 & 0 & 1 & 0 \\ 1 & 0 & -1 & 0 \\ 0 & 1 & 0 & -1 \end{bmatrix} \begin{bmatrix} I_0 \\ I_{45} \\ I_{90} \\ I_{135} \end{bmatrix} \\ &= \begin{bmatrix} 0 & 1 & 0 & 1 \\ 1 & 0 & -1 & 0 \\ 0 & 1 & 0 & -1 \end{bmatrix} \begin{bmatrix} I_0 \\ I_{45} \\ I_{90} \\ I_{135} \end{bmatrix} \\ &= \begin{bmatrix} 0.5 & 0.5 & 0.5 & 0.5 \\ 1 & 0 & -1 & 0 \\ 0 & 1 & 0 & -1 \end{bmatrix} \begin{bmatrix} I_0 \\ I_{45} \\ I_{90} \\ I_{135} \end{bmatrix}. \end{aligned} \quad (8)$$

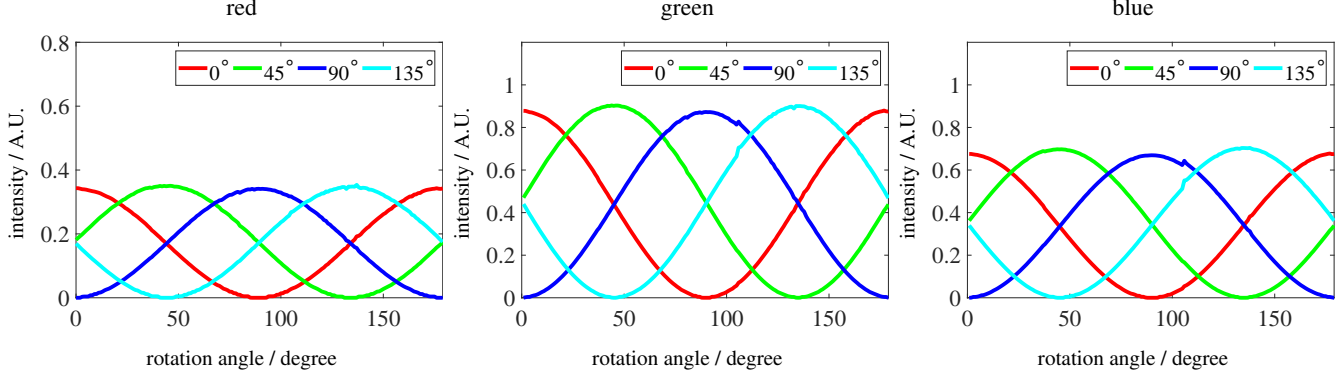


**Figure 1:** Polarization calibration. Intensity changing curves are measured for  $0^\circ$ ,  $45^\circ$ ,  $90^\circ$  and  $135^\circ$  in each color channel (left: red; middle: green; right: blue).

Note that the three forms are equivalent. This is because any light regardless of its polarization states, the electric field can be decomposed into perpendicular components in many different ways as long as the two directions are orthogonal. The total intensity can then be calculated either by  $I_0 + I_{90}$  or  $I_{45} + I_{135}$  or  $0.5(I_0 + I_{90} + I_{45} + I_{135})$ . Mathematically, the matrix in the third line in Eq. (8) is the pseudoinverse of the matrix in Eq. (7). No matter which form to be taken, the product of the two conversion matrices should be an identity matrix. This can easily be validated by substituting Eq. (8) to Eq. (7).

$$\begin{aligned} \mathbb{I} &= \frac{1}{2} \begin{bmatrix} 1 & 0 & 1 & 0 \\ 1 & 0 & -1 & 0 \\ 0 & 1 & 0 & -1 \end{bmatrix} \begin{bmatrix} 1 & 1 & 0 \\ 1 & 0 & 1 \\ 1 & -1 & 0 \\ 1 & 0 & -1 \end{bmatrix} \\ &= \frac{1}{2} \begin{bmatrix} 0 & 1 & 0 & 1 \\ 1 & 0 & -1 & 0 \\ 0 & 1 & 0 & -1 \end{bmatrix} \begin{bmatrix} 1 & 1 & 0 \\ 1 & 0 & 1 \\ 1 & -1 & 0 \\ 1 & 0 & -1 \end{bmatrix} \\ &= \frac{1}{2} \begin{bmatrix} 0.5 & 0.5 & 0.5 & 0.5 \\ 1 & 0 & -1 & 0 \\ 0 & 1 & 0 & -1 \end{bmatrix} \begin{bmatrix} 1 & 1 & 0 \\ 1 & 0 & 1 \\ 1 & -1 & 0 \\ 1 & 0 & -1 \end{bmatrix}. \end{aligned} \quad (9)$$

It is worth noting that the above relationship should always hold. For real polarizers, the conversion matrix from Stokes vector to intensities is

$$P = \frac{1}{2} \begin{bmatrix} k_1^0 + k_2^0 & k_1^0 - k_2^0 & 0 \\ k_1^{45} + k_2^{45} & 0 & k_1^{45} - k_2^{45} \\ k_1^{90} + k_2^{90} & -(k_1^{90} - k_2^{90}) & 0 \\ k_1^{135} + k_2^{135} & 0 & -(k_1^{135} + k_2^{135}) \end{bmatrix}. \quad (10)$$

The conversion matrix from intensities to Stokes vector can be obtained by calculating the pseudoinverse of Eq. (10),

$$Q = P^+. \quad (11)$$

## 2. Calibration

With a high extinction ratio polarizer rotating in front of the polarization sensor, we can assume the input light is perfectly linearly polarized at a specific angle. The reference point for rotation angle and polarization angle are usually not the same, we denote the difference between the two as  $\beta$ . So the Stokes vector for the incident polarized light at rotation angle  $\alpha$  is

$$S_{\text{in}} = \begin{bmatrix} 1 \\ \cos(2(\alpha + \beta)) \\ \sin(2(\alpha + \beta)) \end{bmatrix}. \quad (12)$$

Due to the fabrication errors, the orientation angles for the micropolarizers may be slightly different from their nominal values. The real orientation angle can be expressed as  $\theta + \Delta\theta$ , where  $\Delta\theta$  is the orientation angle error. According to Eq. (4) in the main text, the intensity received on the sensor is

$$I_\theta = (k_1^\theta + k_2^\theta) + (k_1^\theta - k_2^\theta) \cos(2(\theta + \Delta\theta - \alpha - \beta)). \quad (13)$$

We sweep the rotation angle from  $0^\circ$  to  $179^\circ$  with a  $1^\circ$  step, and get the intensity changing curves for the  $0^\circ$ ,  $45^\circ$ ,  $90^\circ$  and  $135^\circ$  micropolarizers. The curves for each color channel are shown in Figure 1. We fit the curves using the following equation

$$f(\alpha) = a_0 + a_1 \cos(2(\theta - \alpha - \beta)). \quad (14)$$

Since we don't know the exact value of  $\beta$ , we take the average of the fitting data as the true value.  $\Delta\theta$  is then calculated as  $\Delta\theta = \theta - \bar{\beta}$ .

Therefore, the calibration matrices for our polarization camera are as follows.

$$\mathbf{P}_r = \begin{bmatrix} 0.4957 & 0.4965 & -0.0011 \\ 0.5073 & 0.0041 & 0.5084 \\ 0.4936 & -0.4939 & 0.0007 \\ 0.5032 & 0.0040 & -0.5026 \end{bmatrix} \quad (15)$$

$$\mathbf{P}_g = \begin{bmatrix} 0.4947 & 0.4937 & -0.0026 \\ 0.5078 & 0.0034 & 0.5065 \\ 0.4925 & -0.4908 & -0.0029 \\ 0.5047 & 0.0029 & -0.5051 \end{bmatrix} \quad (16)$$

$$\mathbf{P}_b = \begin{bmatrix} 0.4924 & 0.4932 & -0.0037 \\ 0.5082 & 0.0045 & 0.5075 \\ 0.4906 & -0.4890 & -0.0049 \\ 0.5083 & 0.0044 & -0.5114 \end{bmatrix} \quad (17)$$

### 3. Polarization Image Dataset

For the four polarization angles  $0^\circ$ ,  $45^\circ$ ,  $90^\circ$  and  $135^\circ$ , we acquire 100 raw images for each angle and average them to get a high signal-to-noise ratio image. We perform color demosaicing with the Matlab `demosaic` function, and then do a  $2 \times 2$  binning to further suppress noise. We get four  $1024 \times 1024$  color images to calculate the total intensity, DoLP and AoLP. The data is provided in the Matlab `.mat` format.

We classify our polarization dataset into roughly four categories of scenarios, as shown in Table 1.

**Table 1:** *Polarization image dataset.*

Category	Scene
laboratory setup	plant, fakefruit, dinosaur, bottles, ball pomegranate, plastik, mirrorcard, tools, plastikcomp mirrorphone, glasscube, funnel, fruit, einstein camera, caligraphset, cablelid, blackstuff, kettle
indoor	woodwall, screen, lock, door, chairs floor, paint, printer, drinkingfountain, monitors
polarized illumination	scotch, plate, glassplasticcomp, glasscontainer, cover penstand, cellphonecases, carrier, ruler, containers

In particular, we would like to point out some typical scenes for polarization test. Since black objects are said very likely to be polarized in the literature, but noise is also very strong in the black surfaces. In order to demonstrate this phenomenon, we show a `blackstuff` scene with all the objects black in color, but in different materials. The exposure time is adjusted to make sure the signal-to-noise ratio is high enough, such that noise can be well suppressed in the scene. We also include a scene of the `einstein` statue, which is almost completely unpolarized. The `door` scene is a good example for polarization from reflection, where the image of the tree on the window is highly polarized, and can be removed by subtracting from the original image (see the Supplementary Video). We categorize cross-polarization as an important polarization scenario, and include 10 images in this category. All the images are taken by placing transparent or translucent objects in front of a computer monitor, which is highly linearly polarized. The intrinsic stress in the objects exhibit strong color fringes when viewed in a polarization camera.

### 4. Visualization

The challenge of visualizing polarization originates from its high dimensionality. Conventional visualization method is to map monochrome polarization image into the HSV color space or other color space to see the polarization effects. In the color polarization case, this method fails because the entire data is now 9D. To address this problem, we propose alternative methods as shown in Fig. 2 to compliment existing visualization methods for color polarization images.

Direct mapping from angle values to gray levels leads to misinterpretation for AoLPs that are close to  $0^\circ$  or  $180^\circ$  – due to angular wraparound similar angles are assigned vastly different intensities. Usually the noisy patterns occur in the AoLPs when there is a large difference between color channels due to angle wraparounds. Thereby it is more reasonable to look at the difference of AoLPs between color channels. We propose to take the AoLP in green channel as a reference, and calculate the absolute difference in blue and red channels with respect to green, resulting in a color image which we call `diffAoLP`. To mitigate the fact that in some cases where `diffAoLP` is rather small and could hardly be seen, we set the green AoLP values as a transparency  $\alpha$  channel to make it more visible. The `diffAoLP` visualizations are shown in Fig. 2 (c) and (h).

Visualizing the polarization state in its entirety is helpful to interpret the whole picture of polarization states. This is particularly reasonable when the DoLP is rather small, where AoLP becomes arbitrary, hence meaningless. In analogy to a vector field within a unit circle, the magnitude links to the value of DoLP, and the direction represents AoLP. Since the wraparound of AoLP happens at  $180^\circ$ , the upper and lower halves of the unit circle are centrosymmetric. Therefore, we can calculate the vector field as  $(\mathbf{u}, \mathbf{v}) = (\mathcal{P} \cos(2\phi), \mathcal{P} \sin(2\phi))$ . We overlay the above vector fields on top of the total intensity component, which is essentially a color image. This makes it possible to show all the 9D information in a single image. As shown in Fig. 2 (d-e) and (i-j), we denote the vector fields with short lines in different colors. The length of the line reflects DoLP, and the orientation of the line indicates AoLP. The color scheme of the lines are chosen in order not to interfere with the original color, but still approximating it. We choose cyan for the blue channel, yellow for green, and white for red. This color scheme is rarely seen in natural objects, but keeps the original color of the image very well, and “pops up” the regions with strong polarization in the meantime. For small DoLPs (less polarized), the vector field becomes a small dot, and hence negligible. The length and orientation differences among the vector fields indicate a noticeable difference of polarization states among color channels. Details can be seen in the zoom-in image. Note that in the `glassplasticcomp` scene, the vector fields exhibit significantly different lengths and orientations among three color channels.

In addition to the above static visualizations, it is even more comprehensive to take advantage of animations to reveal implied information from the underlying polarization states. Since the complete polarization information has been stored in total intensity, DoLP and AoLP, we can synthesize new intensity images with a temporally changing “virtual” polarizer as if the images were taken under the same physical condition, where the virtual linear polarizer can be fully modeled by its Müller matrix. See the Supplementary Video for the virtual polarizer visualization results.

For a thorough review of the both conventional and proposed visualization methods, we show here all the visualization methods in two scenarios: polarized illumination and unpolarized illumination. Figure 3 shows the visualization results for the `blackstuff` scene for unpolarized illumination, and Figure 4 shows the visualization results for the `plate` scene with polarized illumination.

### References

- [Col05] COLLETT E.: *Field guide to polarization*, vol. 15. SPIE press Bellingham, 2005. 1

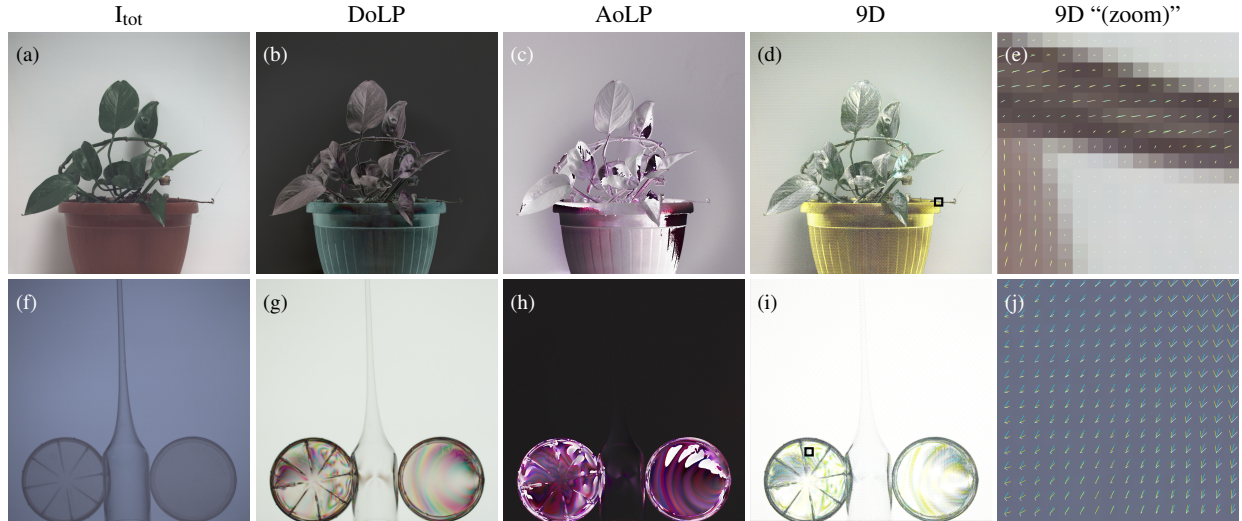


**Figure 2:** Visualization of color polarization for a plant scene with unpolarized illumination and a glassplasticcomp scene with polarized illumination. We show the intensity, DoLP in sRGB color space, AoLP and complete 9D polarization visualization. The zoom-in images on the right show the detailed vector fields indicating the underlying polarization states.

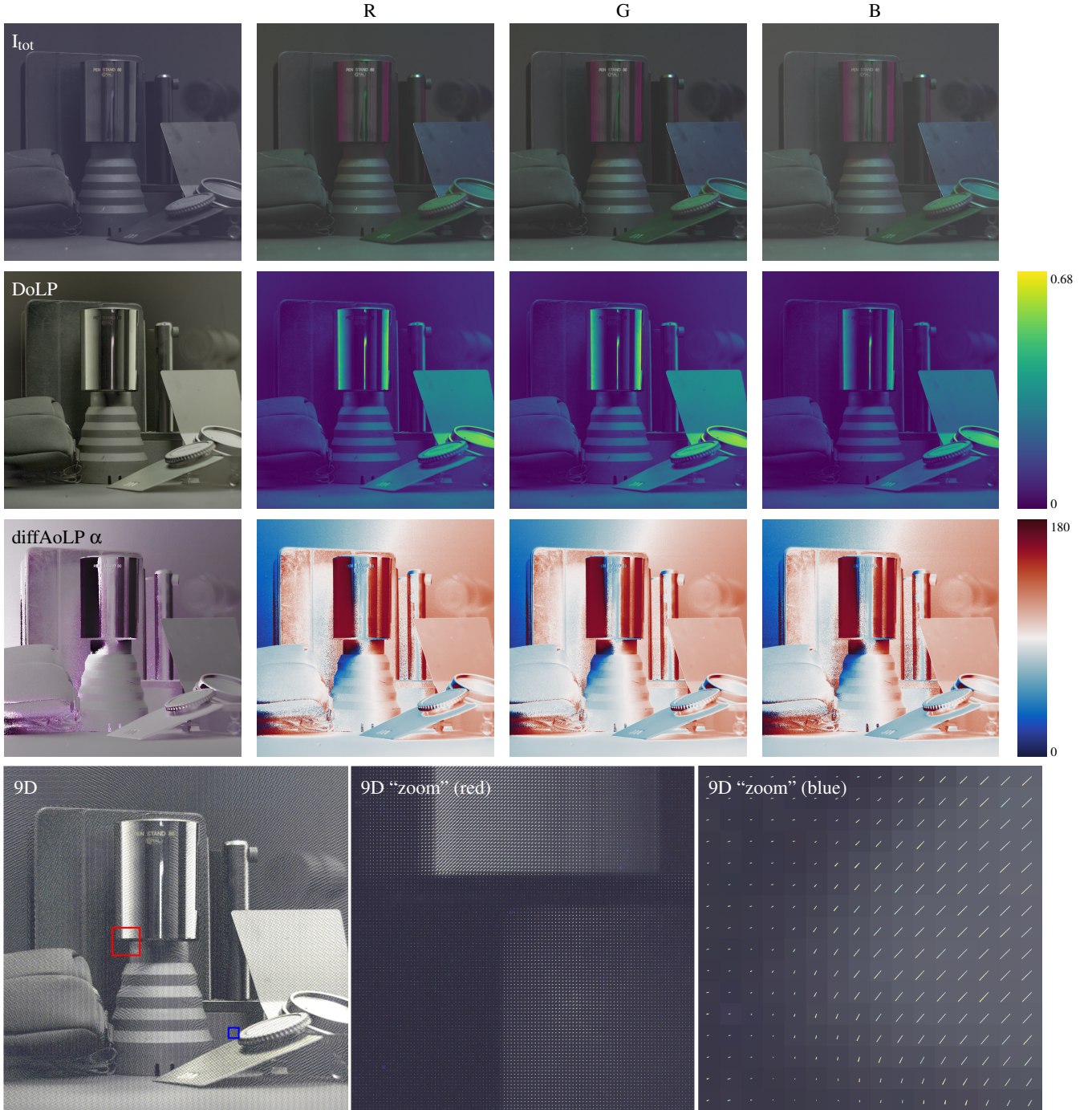


**Figure 3:** All visualization methods for the *blackstuff* scene with natural illumination. The false color image in HSV space for each color channel are shown on the top row, from left to right for R, G and B channels. The intensity images is shown on the right. The second row shows DoLP in false color with the viridis color map. The color bar indicates the DoLP values. Our DoLP in sRGB color space is shown on the right. The third row shows AoLP in false color for each color channel, with the cmocean “balance” color map. Our diffAoLP with transparency channel is shown on the right. The bottom row shows the 9D color polarization information. Zoom-ins show the details in the scene. Polarization among color channels are pretty the same.

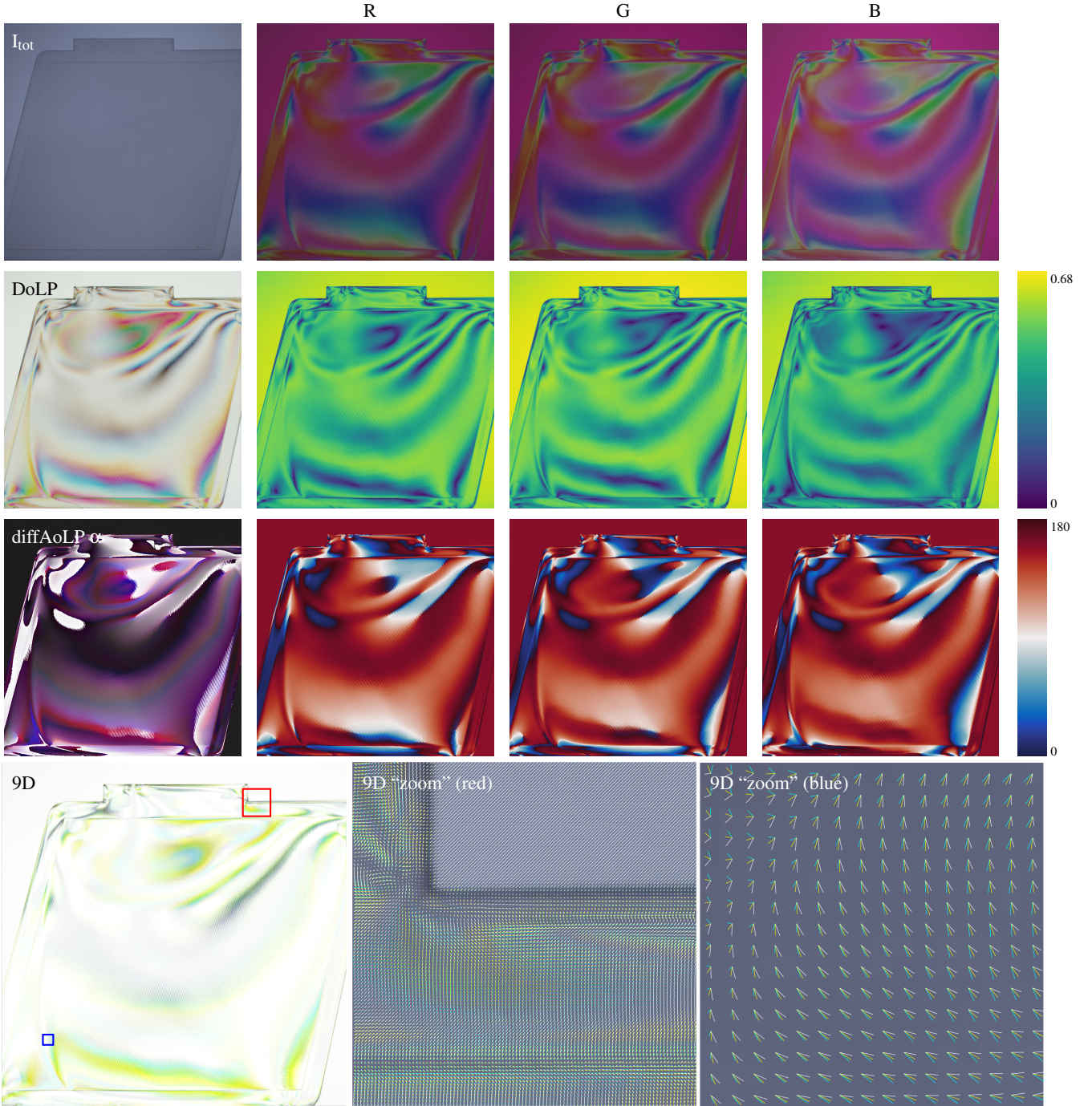


**Figure 4:** All visualization methods for the plate scene for cross-polarization. The false color image in HSV space for each color channel are shown on the top row, from left to right for R, G and B channels. The intensity images is shown on the right. The second row shows DoLP in false color with the viridis color map. The color bar indicates the DoLP values. Our DoLP in sRGB color space is shown on the right. The third row shows AoLP in false color for each color channel, with the cmocean ‘balance’ color map. Our diffAoLP is shown on the right. The bottom row shows the 9D color polarization information. Zoom-ins show the details in the scene. The difference in the vector fields shows the significant polarization difference among color channels.